Characterization of Recombinant Horseradish Peroxidase C and Three Site-Directed Mutants, F41V, F41W, and R38K, by Resonance Raman Spectroscopy†

Giulietta Smulevich,*,‡ Mauro Paoli,‡ Julian F. Burke,§ Stephen A. Sanders,§ Roger N. F. Thorneley,∥ and Andrew T. Smith§

Dipartimento di Chimica, Università di Firenze, Via G. Capponi 9, 50121 Firenze, Italy, and Biochemistry Laboratory and AFRC-IPSR Nitrogen Fixation Laboratory, University of Sussex, Brighton, U.K.

Received January 11, 1994; Revised Manuscript Received March 31, 1994®

ABSTRACT: Resonance Raman spectra are reported for recombinant horseradish peroxidase C (HRP-C*) and three protein variants prepared by *in vitro* refolding after *Escherichia coli* expression. The spectra of their Fe^{II} and Fe^{III} forms and of their complexes with benzohydroxamic acid (BHA) were recorded at neutral pH. The residues mutated were on the distal [Phe41→Trp or Val (F41W, F41V) and Arg38→Lys (R38K)] side of the heme. The spectra give information on the spin and ligation states via the frequencies of the core size marker bands. No detectable modification in the enzyme structure or in the heme group has been observed in the wild-type recombinant HRP-C*. The Fe^{III} forms of both the recombinant and the plant proteins show the coexistence of a 5-(5-cHS) and a 6-coordinate high-spin (6-cHS) heme, characterized by the anomalous frequencies of certain bands, namely, ν_3 and ν_{10}, which we attribute to a different degree of distortion of the heme planarity with respect to other heme proteins and model compounds, resulting from external forces such as steric contacts within the protein. This effect is partially relieved upon complexation with BHA or as a result of mutation. F41W and F41V are characterized by an increase in a 6-cHS form at the expense of the 5-cHS species, and the R38K by an increase in both the 6-c high-(HS) and low-spin (LS) hemes. The 6-cHS and -LS species are characterized by normal core size marker band frequencies. The Fe^{II}–His RR band is at 243 cm^{-1} in HRP-C*, the high frequency value being due to hydrogen-bonding interactions between the proximal His170 N_δ and the carboxylate acceptor group on Asp247. Mutation at position 38 causes a downshift of 3 cm^{-1} in the ν(Fe–Im) stretching mode, suggesting a weakening of the Fe–Im bond strength. By comparing the results obtained with HRP-C* mutants with those previously reported for the corresponding cytochrome *c* peroxidase (CCP) mutants, it appears that the distal heme pocket architecture is significantly different in the two peroxidases, although the hydrogen-bonding network coupling the distal and the proximal sides of the heme appears to be conserved. Mutations on the distal side dramatically affect the capability of the protein to bind BHA. F41W and R38K mutants do not bind the substrate, whereas the F41V variant shows a 2-fold increase in affinity. The data are consistent with the current model of the BHA binding site lying toward the distal rather than the proximal side of the heme.

Peroxidases are a commercially and environmentally important class of enzymes that, in their resting state, contain a 5-coordinate high-spin heme prosthetic group. Collectively, they catalyze the oxidation by hydrogen peroxide of a diverse range of substrates that include cytochrome *c*, organic dyes, substituted phenols, anilines (Sakurada *et al.*, 1990), and some of the more electronegative methoxybenzenes (Kersten *et al.*, 1990). By applying a combination of structural, kinetic, and spectroscopic techniques to wild-type and recombinant mutant forms of these relatively small proteins (M = 30000–40000), it is possible to begin to understand how the reactivity of the heme is modulated by the protein environment.

Two of the best characterized peroxidases are cytochrome *c* peroxidase (CCP[1]) (Bosshard *et al.*, 1991; Smulevich, 1993) and horseradish peroxidase C (HRP-C) (Dunford & Stillman, 1976; Dunford, 1991). In the context of the present paper, resonance Raman spectroscopy has been extensively applied to wild-type and variant CCP proteins (Smulevich et al., 1988a,b, 1989a,b, 1990a,b, 1991a). Changes in the frequencies of the bands above 1450 cm^{-1} due to the porphyrin skeletal vibrational modes were used to detect changes in heme spin and ligation states resulting from single site mutations in the heme pocket of the protein. The recent development of procedures for the recovery of active recombinant enzyme by *in vitro* refolding after *Escherichia coli* expression (Smith *et al.*, 1990, 1992, 1993) and the construction of protein variants of HRP-C is allowing, for the first time, a range of spectroscopic (Veitch *et al.*, 1992), kinetic (Smith *et al.*, 1992,

†This work was supported by grants from the Italian Consiglio Nazionale delle Ricerche (CNR) and Ministero Università e Ricerca Scientifica e Tecnologica (MURST) (to G.S. and M.P.), the Science and Engineering (SERC) and Agriculture and Food (AFRC) Research Councils under the Transition Metals in Biology and Coordination Chemistry Programme (to A.T.S., J.F.B., R.N.F.T.), and the EEC Human Capital and Mobility Programme "Peroxidases in Agriculture and the Environment" [ERB CHRX-CT92-0012-130]. S.A.S. was supported by a SERC studentship.

* Author to whom correspondence should be addressed.
‡ Università di Firenze.
§ Biochemistry Laboratory, University of Sussex.
∥ AFRC-IPSR Nitrogen Fixation Laboratory, University of Sussex.

® Abstract published in *Advance ACS Abstracts,* May 15, 1994.

[1] Abbreviations: HRP-C, horseradish peroxidase isoenzyme C; HRP-C*, recombinant horseradish peroxidase isoenzyme C; F41V, Phe41→Val HRP-C* mutant; F41W, Phe41→Trp HRP-C* mutant; R38K, Arg38→Lys HRP-C* mutant; CCP, cytochrome *c* peroxidase; CCP(MI), cytochrome *c* peroxidase expressed in *E. coli*; BHA, benzohydroxamic acid; ABTS, 2,2′-azinobis(3-ethylbenzothiazolinesulfonic acid); MOPS, 3-morpholinopropanesulfonic acid; 5-cHS, 6-cHS, and 6-cLS, 5- and 6-coordinate high- and low-spin, respectively; RR, resonance Raman; NMR, nuclear magnetic resonance.

0006-2960/94/0433-7398$04.50/0

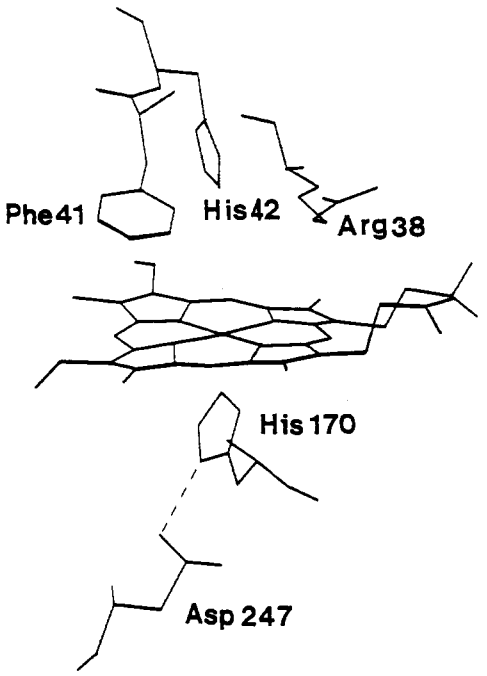

FIGURE 1: Schematic representation of the heme active site of HRP-C based on the modeling studies (Smith *et al.*, 1993).

1993; Sanders *et al.*, 1994), and crystallographic (Henriksen *et al.*, 1993) studies complementary to those previously published for CCP.

The high-resolution X-ray structures of baker's yeast CCP (Poulos & Kraut, 1980; Finzel *et al.*, 1984) led Poulos and Kraut (1980) to propose a general acid/base catalysis mechanism for hydrogen peroxide binding and reduction, with essential roles for two highly conserved residues in the distal heme pocket (Arg48 and His52). The equivalent residues in HRP-C are Arg38 and His42 (Figure 1). The CCP variants, R48K and R48L, react with hydrogen peroxide to form compound I 2- and 200-fold slower, respectively, than does native CCP (Erman *et al.*, 1992). The compound I forms of these variants were also found to be much less stable with respect to autoreduction to the ferric enzyme. It was concluded that a basic residue at position 48 in CCP is not an obligate requirement for the formation of a ferryl intermediate and that the distal His plays a far more significant role (Erman *et al.*, 1992). In contrast, the R38K variant of HRP-C showed a 500-fold decrease in the rate of compound I formation (Smith *et al.*, 1993). Therefore in CCP, a lysine residue is able to substitute quite well for arginine 48 with respect to compound I formation, but is not able to do so nearly as efficiently at arginine 38 in HRP-C.

Significant differences are observed in the degree to which the Arg→Lys substitution is tolerated in the two enzymes, presumably related to differences in their heme pocket architectures. Recent data (Smith *et al.*, 1993) suggest that part of the role of the conserved Arg in wild-type HRP-C is to ensure that compound I formation is an essentially irreversible reaction proceeding to completion at low concentrations of peroxide. It is because CCP has been the accepted paradigm for the plant peroxidases that in comparative studies of HRP-C variants it is important to recognize any functional differences and establish their structural origins. Although a high-resolution structure is not currently available for HRP-C, careful comparisons of the sequence data for the plant and fungal peroxidase superfamily with those for CCP have shown that the overall protein fold is probably similar (Welinder, 1985, 1992). This prediction recently was confirmed by a low-resolution tertiary structure of HRP-E5 (Morita *et al.*, 1991, 1993) and by the more recent structures of ligninase (Edwards *et al.*, 1993; Poulos *et al.*, 1993; Piontek *et al.*, 1993) and a peroxidase from *Arthromyces ramosus* (Kunishima *et al.*, 1994).

The key catalytic residues in HRP-C (His42, Arg38, and His170) (Figure 1) and in CCP (His52, Arg48, and His175) are highly conserved (Welinder, 1992). Furthermore, ^{1}H NMR studies of HRP-C (de Ropp *et al.*, 1984, 1991; de Ropp & La Mar, 1991; Thanabal *et al.*, 1987a,b, 1988) have provided evidence that the imidazolate nature of the axial ligand and the general dispositions of His42 and Arg38 with respect to the heme are similar between HRP-C and CCP. However, resonance Raman has shown as yet unexplained differences between the heme core size marker bands of these two peroxidases that have not previously been highlighted in the literature. Despite this, the heme Fe atom of HRP-C has been assigned as 5-coordinate high-spin (Rakshit & Spiro, 1974; Teraoka & Kitagawa, 1981; Kitagawa *et al.*, 1983; Terner & Reed, 1984; Evangelista-Kirkup *et al.*, 1985; Palaniappan & Terner, 1989; Smulevich *et al.*, 1991b). In addition, the two proteins give rise to different species at low temperature: CCP undergoes conversion to a 6-coordinate low-spin heme at 10 K (Yonetani & Anni, 1987; Smulevich *et al.*, 1989b), whereas HRP-C shows an intermediate-spin heme (Maltempo *et al.*, 1979; Evangelista-Kirkup *et al.*, 1985; Smulevich *et al.*, 1991b). This behavior also suggests differences in the heme protein environment of the two enzymes.

In a recent paper, Veitch *et al.* (1992) examined the ^{1}H NMR spectra of recombinant HRP-C (HRP-C*) and two protein variants, F41V and R38K. The spectrum of native plant enzyme, with the exception of the carbohydrate-linked resonances, was essentially identical to that of the refolded recombinant enzyme. Comparison of the spectra of the cyanide-ligated states of the wild-type and the two protein variants indicated that there were significant differences with respect to the heme and heme-linked resonances. In particular, mutations on the distal side of the heme were able to influence the degree of imidazolate character of the axial histidine. Similar effects previously had been observed for the corresponding CCP mutants by resonance Raman (Smulevich *et al.*, 1991a). A structural explanation for this effect, in the case of the CCP R48L variant, has been proposed to involve coupling between distal and proximal residues by means of an extended hydrogen-bonding network (Smulevich *et al.*, 1988a, 1991a).

In this paper, we report the characterization by resonance Raman spectroscopy of three HRP-C* variants, including Arg38→Lys (R38K), Phe41→Val (F41V), and Phe41→Trp (F41W) in both their ferrous and ferric states and after complex formation with benzohydroxamic acid (BHA). The Phe41 variants are important because all but three of the current 23 members of the plant peroxidase superfamily contain a Phe at position 41 (HRP numbers). The exceptions are CCP, pea ascorbate peroxidase, and *E. coli* peroxidase, which contain a Trp at this position (Welinder, 1992). We compare our observations of the effects of these mutations on the heme iron spin and coordination state of HRP-C with those previously reported for the corresponding CCP mutants. We present evidence that the heme pocket architectures of HRP-C and CCP are significantly different, although the hydrogen-bonding network coupling the distal and proximal sides of the heme appears to be conserved.

EXPERIMENTAL PROCEDURES

Construction of Mutant HRP-C Genes.* A polymerase chain reaction (PCR)-based technique with the HRP-C

synthetic gene (Smith *et al.*, 1990) as template was used to generate insert DNA bearing the required mutations. The construction of the F41V and R38K mutations has been described elsewhere (Smith *et al.*, 1992). For the F41W mutation, the polymerase chain reaction was performed as previously described for the F41V mutation, except that oligonucleotide T2 replaced V1. T2 was identical to the wild-type synthetic gene sequence between nucleotide positions 111 and 144, except that it contained the Trp codon TGG at position 135 (5′GCTGCTTCAATATTACGTCTGCACTG-GCATGAC3′). Amplified DNA fragments (371 bp) bearing the mutation were cloned in-frame into the wild-type gene at the unique *Ssp*1 and *Xho*1 sites in the HRP expression vector pAS5 (Smith *et al.*, 1992). Double-stranded DNA sequence analysis by the dideoxy chain termination method, using sequenase version 2 (Saunders & Burke, 1990) and oligonucleotides S1 and V1 (Smith *et al.*, 1992) as sequencing primers, confirmed the expected sequence changes.

Preparation of Recombinant Peroxidase. Growth and induction of *E. coli* strains producing recombinant peroxidase variants were as previously described (Smith *et al.*, 1992). Folding and activation of HRP-C* recovered from *E. coli* inclusion bodies were achieved essentially by the method of Smith *et al.* (1990), with the modifications subsequently described by Smith *et al.* (1992). Purified enzyme was desalted into 10 mM sodium MOPS (pH 7.1) and stored in liquid nitrogen. Samples were concentrated just before use to 0.2–0.4 mM for Raman spectroscopy employing Soret band excitation and to 1 mM for excitation in the visible region. Peroxidase concentrations were determined using the Soret extinction coefficients determined by the pyridine hemochrome method as reported in Smith *et al.* (1992). These were 102 mM^{-1} cm^{-1} for HRP-C* (Dunford & Stillman 1976), 124 mM^{-1} cm^{-1} for F41V (Smith *et al.*, 1992), 113 mM^{-1} cm^{-1} for F41W (previously unpublished result), and 125 mM^{-1} cm^{-1} for R38K (Sanders *et al.*, 1994). The specific activities and RZ (Reinheitszahl) values of the horseradish peroxidase preparations used in this work were 930 units mg^{-1} and 3.2 for HRP-C*, 230 units mg^{-1} and 3.7 for F41V, 58 units mg^{-1} and 3.0 for F41W, and 64 units mg^{-1} and 2.9 for R38K, respectively. Activities were measured as previously described with 0.3 mM ABTS and 2.5 mM H_2O_2 (Smith *et al.*, 1990).

Preparation of Samples for Resonance Raman Spectroscopy. The Fe^{III} forms were dissolved in 5 mM sodium MOPS buffer at pH 7.1. The Fe^{II} forms were prepared by adding a 2-μL volume of dithionite solution (20 mg mL^{-1}) to 100 μL of deoxygenated peroxidase solution, and the redox state was checked by recording a UV/visible absorption spectrum. Aromatic donor complexes with benzohydroxamic acid (BHA, Sigma) were made by adding BHA (25 mM) to give the required final concentration in 10 mM sodium MOPS buffer at pH 7.1. The dissociation constants (K_d) for BHA are 2.6 and 1.1 μM with HRP-C* and the F41V variant, respectively (Smith *et al.*, 1992).

Resonance Raman Spectroscopy. Resonance Raman spectra were obtained at room temperature with excitation from a Kr^+ laser (Coherent, Innova 90/K) using the 406.7-, 530.9-, and 568.2-nm lines and from an Ar^+ laser (Coherent, Innova 90/5) using the 457.9-, 496.5-, and 514.5-nm lines. The back-scattered light from a slowly rotating NMR tube was collected and focused into a computer-controlled double monochromator (Jobin-Yvon HG 2S) equipped with a cooled photomultiplier (RCA C31034 A) and photon counting electronics. The RR spectra were calibrated to an accuracy of 2 cm^{-1} for intense isolated bands, with indene as standard (Hendra & Loader, 1968) for the high-frequency region and with indene and CCl_4 for the low-frequency region. Polarized spectra were obtained by inserting a polaroid analyzer between the sample and the entrance slit of the spectrometer. The polarization of the bands at 318 and 459 cm^{-1} of CCl_4 was measured to check the reliability of the polarization measurements using a rotating NMR tube with 180° back-scattered geometry. The values of the depolarization ratios, $\rho = 0.73$ and 0, respectively, compared favorably with the theoretical values of 0.75 and 0. In order to evaluate band intensities, spectra were simulated with a band-fitting program using Lorentzian line shapes.

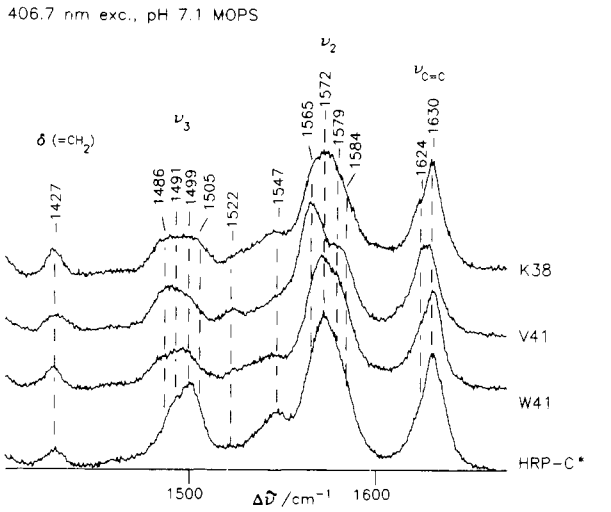

FIGURE 2: Resonance Raman spectra of Fe^{III} recombinant HRP-C* and the R38K, F41V, and F41W variants at pH 7.1 recorded with 406.7-nm excitation. Experimental conditions: 5-cm^{-1} resolution; 6 s/0.5 cm^{-1} collection interval; and 30-mW laser power at the sample.

RESULTS

Effect of HRP-C Mutations on Heme Iron Spin and Coordination States.* The high-frequency regions of the resonance Raman spectra (RR) of HRP-C* variants and the wild type obtained with B-band (Soret) excitation are shown in Figure 2. The spectrum of the refolded, recombinant (wild-type) enzyme produced from *E. coli* (HRP-C*) was identical to that previously reported for the commercially available glycosylated plant enzyme (HRP-C) (Rakshit & Spiro, 1974; Teraoka & Kitagawa, 1981; Kitagawa *et al.*, 1983; Terner & Reed, 1984; Evangelista-Kirkup *et al.*, 1985; Palaniappan & Terner, 1989; Smulevich *et al.*, 1991b). These data confirm the high degree of similarity between the two enzyme forms previously concluded from electronic absorption (Smith *et al.*, 1992) and ^1H NMR data (Veitch *et al.*, 1992). In contrast, single residue substitutions in the distal heme pocket (see the sketch of the active site in Figure 1) had a marked effect on the RR spectra. Figure 2 shows that each of the three distal site substitutions caused a broadening of the band in the ν_3 region.

As previously reported for HRP-C, the ν_3 region contains two characteristic bands at 1491 and 1499 cm^{-1} assigned to two species corresponding to 6-coordinate high-spin (6-cHS) and 5-coordinate high-spin (5-cHS) hemes, respectively (Smulevich *et al.*, 1991b). All three distal site variants contained an extra band on the low-frequency side of the ν_3 region at about 1486 cm^{-1}, corresponding to a 6-cHS form (Choi *et al.*, 1982). The corresponding bands in both the ν_2 and ν(C=C) regions, due to a 6-cHS heme, are also seen in all of the variants at 1565 and 1624 cm^{-1}, respectively. The effect is particularly marked for the F41V variant. In addition, R38K is characterized by an extra band at 1505 cm^{-1} in the

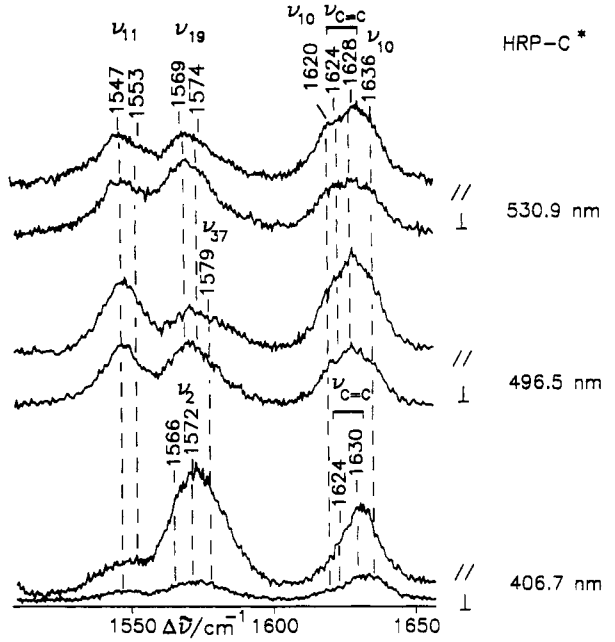

FIGURE 3: Resonance Raman spectra of Fe^{III} recombinant HRP-C* at pH 7.1 recorded in polarized light at various excitation wavelengths. Experimental conditions: 5-cm^{-1} resolution; 406.7-nm excitation, 5 s/0.5 cm^{-1} collection interval, and 40-mW laser power at the sample; 496.5-nm excitation, 18 s/0.5 cm^{-1} collection interval, and 70-mW laser power at the sample; 530.9-nm excitation, 30 s/0.5 cm^{-1} collection interval, and 70-mW laser power at the sample.

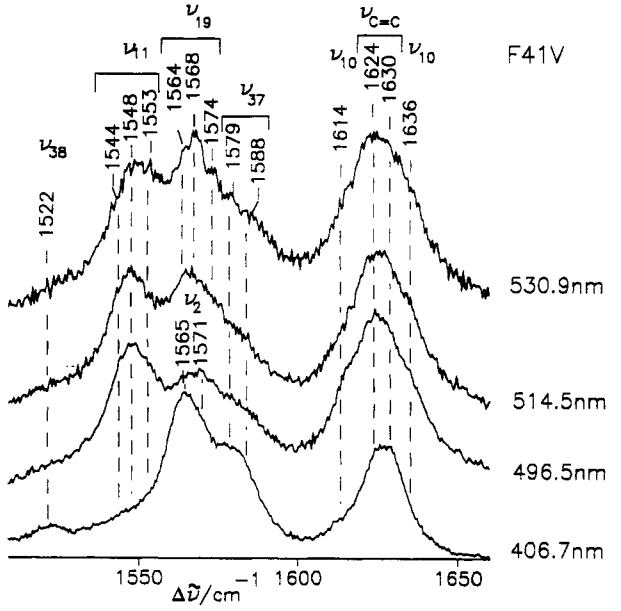

FIGURE 4: Resonance Raman spectra of the Fe^{III} F41V variant at pH 7.1 recorded at various excitation wavelengths. Experimental conditions: 5-cm^{-1} resolution; 406.7-nm excitation, 3 s/0.5 cm^{-1} collection interval, and 30-mW laser power at the sample; 496.5-nm excitation, 24 s/0.5 cm^{-1} collection interval, and 70-mW laser power at the sample; 514.5-nm excitation, 22 s/0.5 cm^{-1} collection interval, and 70-mW laser power at the sample; 530.9-nm excitation, 20 s/0.5 cm^{-1} collection interval, and 70-mW laser power at the sample.

ν_3 region and an additional shoulder in the ν_2 region at 1584 cm^{-1}. These features are typical of a low-spin heme state (Choi *et al.*, 1982).

The polarized spectra of HRP-C* at different excitation wavelengths are shown in Figure 3. With Soret excitation (406.7 nm), polarized bands (p) are seen corresponding to the ν_2 (A_{1g}) (1566 and 1572 cm^{-1}) and vinyl (1624 and 1630 cm^{-1}) modes (Choi *et al.*, 1982), as previously reported (Rakshit & Spiro, 1974). Careful inspection of the spectrum reveals a new depolarized band (dp) at 1636 cm^{-1}, which is more intense with visible excitation (Figure 3). This is because with Q-band excitation the non totally symmetric vibrational modes of the heme are resonance-enhanced via the B-term (vibronic mixing) mechanism (Spiro & Li, 1988). This also explains why with 530.9-nm excitation prominent depolarized bands are also seen. These were therefore assigned to the B_{1g} porphyrin skeletal modes: ν_{10} (1620 and 1636 cm^{-1}) and ν_{11} (1547 cm^{-1}). An inverse polarized band (ip) at 1569 cm^{-1} was assigned to the ν_{19} (A_{2g}) mode, and a polarized band at 1579 cm^{-1} was assigned to the ν_{37} (E_u) mode.

It is interesting to note that, with Q-band excitation, the ν(C=C) (vinyl) stretching modes are still seen as polarized bands and overlap with the ν_{10} mode, even though they are not expected *a priori* to be enhanced with visible excitation. HRP-C is not the only example of this behavior since both CCP single-crystal and solution RR have shown a strong ν(C=C) band with 514.5-nm excitation (Smulevich, 1990a). This has complicated the interpretation of such data and led previous workers (Rakshit & Spiro, 1974; Teraoka & Kitagawa, 1981; Kitagawa *et al.*, 1983; Palaniappan & Terner, 1989; Smulevich *et al.*, 1991b) to misassign the band at 1630 cm^{-1} to the ν_{10} skeletal mode. However, on the basis of the data in polarized light shown in Figure 3, we can confidently assign the band at 1630 cm^{-1} to the ν(C=C) mode and the band at 1636 cm^{-1} to the ν_{10} mode. Clearly, the vinyl modes are coupled, via anharmonic terms of the potential, to the ν_{10} mode, the slight shift in frequency (1630 to 1628 cm^{-1}, Figure 3) on Q-band excitation being consistent with this coupling.

The new assignments based on the present results (Figure 3) are summarized in Table 1. Note that many of the core size marker bands of HRP are split into two components, suggesting that two forms of HRP are present. These are referred to as 5-cHS# and 6-cHS# in Table 1, where the # indicates that the frequencies of the core size marker bands differ from those generally recognized as arising from 5-cHS and 6-cHS hemes in model compounds (Choi *et al.*, 1982), CCP (5-cHS; Smulevich *et al.*, 1988a,b), or metmyoglobin F complex (6-cHS; Choi *et al.*, 1982) (see below).

Figure 4 shows the RR spectra of the F41V variant obtained at different excitation frequencies. On the basis of these data and also measurements in polarized light (data not shown), new bands are observed with Q excitation at 1544 (shoulder) and 1614 cm^{-1}. Both are depolarized and are therefore assigned to the ν_{11} and ν_{10} modes of a "normal" 6-cHS heme, in agreement with the frequency of the ν_3 band (1486 cm^{-1}) observed with Soret excitation (Figure 2).

Figure 5 shows the RR spectra of the R38K variant recorded with different excitation wavelengths. Besides the modes due to the 6-cHS heme, which are identical with those observed for F41V (see Figure 4), new bands at 1586 (ip) and 1642 cm^{-1} (dp) appear with Q-band excitation. These bands are assigned, on the basis of their polarization behavior (data not shown), to the ν_{19} and ν_{10} modes of a 6-cLS heme.

Figure 6 shows the RR spectra of the F41W variant obtained with different excitation wavelengths. By comparing these results with those of R38K, it can be seen that this variant also contains normal 6-cHS heme and a very small amount of low-spin heme, although less than in R38K.

Effect of BHA on the Resonance Raman Spectra of HRP-C Variants. Figure 7 shows the RR spectra of HRP-C* and its variants obtained with Soret excitation in the presence of saturating BHA. By comparison with the spectra in Figure 2, it can be seen that BHA considerably affected the spectra of the recombinant wild type and the F41V variant, but had

Table 1: Observed Resonance Raman Band Frequencies (cm^{-1}) for HRP-C*, Its Mutant, and Their Complexes with BHA[a]

			HRP-C*		HRP:BHA		V41			V41:BHA		W41				K38			
mode	sym	pol	6-c HS#	5-c HS#	6-c HS	6-c HS#	6-c HS	6-c HS#	5-c HS#	6-c HS	6-c HS#	6-c HS	6-c HS#	5-c HS#	6-c LS	6-c HS	6-c HS#	5-c HS#	6-c LS
$\delta(=CH_2)$		p	1427		1427		1427			1427		1427				1427			
n_3	A_{1g}	p	1491	1499	1486	1491	1486	1491	1499	1486	1491	1486	1491	1499		1486	1491	1499	1505
ν_{38}	E_u	p					1522			1521									
ν_{11}	B_{1g}	dp	1547	1553	1543		1544	1548	1553	1544		1546		1553		1544	1548	1553	
ν_2	A_{1g}	p	1566	1572	1567		1565		1571	1563		1566		1571		1566		1572	1578
ν_{19}	A_{2g}	ip	1569	1574	1564		1564	1568	1574	1561		1568				1569		1575	1586
ν_{37}	E_u	p	1579	1584	1579		1579		1588	1579		1579		1588		1579			
ν(C=C)		p	1624		1624		1624			1624		1624				1623			
ν(C=C)		p	1630		1631		1630			1630		1631				1630			
ν_{10}	B_{1g}	dp	1620	1636	1617		1614		1636	1614		1620		1635	1642	1614		1636	1642

[a] 5-cHS, 6-cHS, and 6-cLS: 5-coordinate high-spin, 6-coordinate high-spin, and 6-coordinate low-spin hemes, respectively. # identifies the hemes that differ for the frequency of some core size marker bands with respect to model compounds (see text). sym, symmetry; pol, polarization.

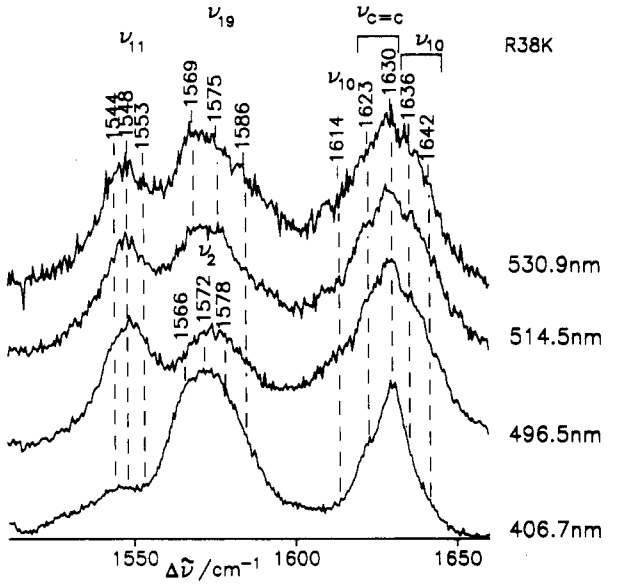

FIGURE 5: Resonance Raman spectra of the Fe^{III} R38K variant at pH 7.1 recorded at various excitation wavelengths. Experimental conditions: 5-cm^{-1} resolution; 406.7-nm excitation, 6 s/0.5 cm^{-1} collection interval, and 30-mW laser power at the sample; 496.5-nm excitation, 44 s/0.5 cm^{-1} collection interval, and 70-mW laser power at the sample; 514.5-nm excitation, 30 s/0.5 cm^{-1} collection interval, and 70-mW laser power at the sample; 530.9-nm excitation, 32 s/0.5 cm^{-1} collection interval, and 70-mW laser power at the sample.

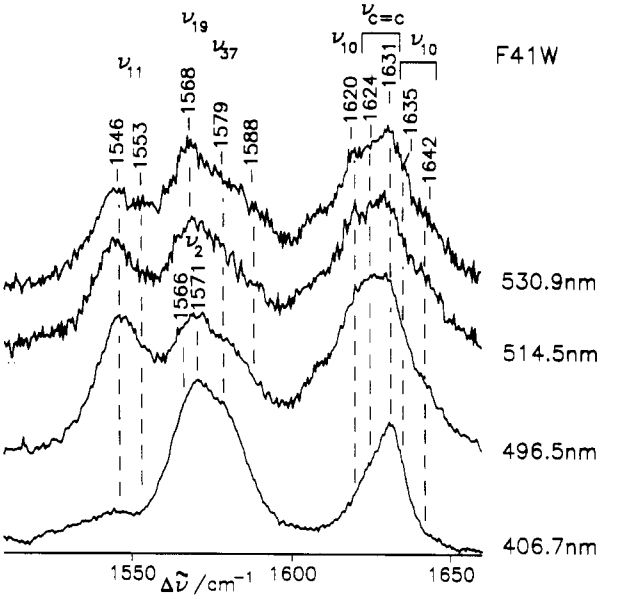

FIGURE 6: Resonance Raman spectra of the Fe^{III} F41W variant at pH 7.1 recorded at various excitation wavelengths. Experimental conditions: 5-cm^{-1} resolution; 406.7-nm excitation, 6 s/0.5 cm^{-1} collection interval, and 30-mW laser power at the sample; 496.5-nm excitation, 45 s/0.5 cm^{-1} collection interval, and 70-mW laser power at the sample; 514.5-nm excitation, 10 s/0.5 cm^{-1} collection interval, and 70-mW laser power at the sample; 530.9-nm excitation, 32 s/0.5 cm^{-1} collection interval, and 70-mW laser power at the sample.

no significant effect on the spectra of the R38K and F41W variants. Similar observations have been made for the visible spectra of these variants (S. A. Sanders and A. T. Smith, unpublished observations).

The behavior of HRP-C* with BHA was very similar to that reported previously for the plant enzyme (Teraoka & Kitagawa, 1981; Kitagawa *et al.*, 1983; Smulevich *et al.*, 1991b). BHA induced the appearance of new bands characteristic of a normal 6-cHS species at 1486 and 1566 cm^{-1} and a shoulder at around 1614 cm^{-1}, which were assigned to the ν_3, ν_{11}, and ν_{10} modes, respectively. The increase in the proportion of the 6-cHS form appeared to be largely at the expense of the 5-cHS# form. In contrast, the 6-cHS# form was unaffected by the addition of BHA. The same changes were observed in the spectrum of F41V after the addition of BHA (Figure 7), except that an even higher proportion of the heme iron was found to be in the 6-cHS form. The spectra of HRP-C* and the F41V variant also differ in the relative intensities of the two ν(C=C) stretching modes observed at 1630 and 1624 cm^{-1}, the latter being much more intense in F41V and positively correlated with the appearance of the 6-cHS form. The enhancement of the 1624 cm^{-1} band on BHA binding has been noted previously for the plant enzyme (Smulevich *et al.*, 1991b). This may, in part, be due to the overlap between the 1624 cm^{-1} band assigned to the ν(C=C) mode and the pronounced shoulder at 1614 cm^{-1} arising from the ν_{10} mode of the 6-cHS heme form.

Analysis of the data in Figure 7 shows a clear difference between the wild-type recombinant and the F41V variant in the contribution of the 1573 cm^{-1} band to the intensity of the ν_2 region. Since the 1573 cm^{-1} band is attributed to the 5-cHS# form, this strongly suggests that the F41V variant with BHA bound contains less 5c-HS# than does native HRP-C with BHA bound, i.e., for the native enzyme, binding of BHA does not convert all of the 5-cHS# form to 6-cHS. The ν_3 regions of the spectra (Figure 7), together with the resulting line shapes obtained from a band-fitting program using Lorentzian components (Figure 8), are consistent with this conclusion.

Figure 9 shows the RR spectra, obtained with different excitation wavelengths, of the BHA complexes of HRP-C* and the F41V variant. With visible excitation, the F41V variant shows bands at 1544, 1561, 1563, and 1614 cm^{-1}. These correspond very well with those observed for model compounds and are assigned to the ν_{11}, ν_{19}, ν_2, and ν_{10} modes

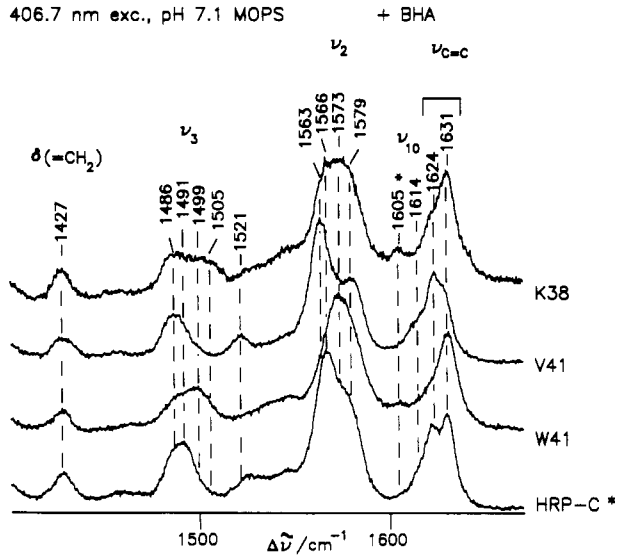

FIGURE 7: Resonance Raman spectra of the BHA-complexed forms of recombinant HRP-C* and the R38K, F41V, and F41W variants at pH 7.1, with excitation at 406.7 nm, 5-cm^{-1} resolution, a 4 s/0.5 cm^{-1} collection interval, and 30-mW laser power at the sample. The * indicates the band at 1605 cm^{-1} due to BHA.

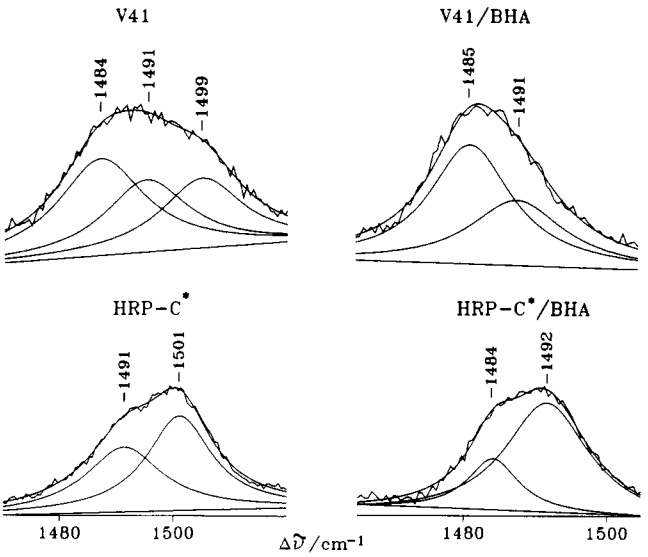

FIGURE 8: Resonance Raman and curve-fitted spectra in the ν_3 region of HRP-C*, the F41V variant, and their complexes with BHA obtained with 406.7-nm excitation. Experimental conditions are as given in the legend to Figure 7.

of a 6-cHS heme, respectively (Choi *et al.*, 1982). These data confirm the presence of almost pure 6-cHS heme in the F41V:BHA complex. In contrast, the corresponding frequencies for native HRP-C are slightly higher, especially for the ν_{19}, ν_2, and ν_{10} bands, which occur at 1564, 1567, and 1617 cm^{-1}, respectively. These data confirm the presence of a mixture of two heme species, both hexacoordinated but possibly differing in their degree of distortion from a planar conformation. There is no evidence for any pentacoordinate species present when BHA is bound to the F41V variant, although a small amount may remain in the HRP-C*:BHA complex.

The F41V variant and HRP-C* both exhibit two ν(C=C) stretching modes at 1624 and 1630 cm^{-1}, with both visible and Soret excitation (see above). In order to confirm these assignments, RR spectra were recorded for the HRP-C*:BHA complex in polarized light with both 406.7- and 530.9-nm excitation (Figure 10). The resulting spectra were simulated using a Lorentzian line shape band-fitting program with an 11.2 cm^{-1} bandwidth for the band at 1616 cm^{-1} and a 10 cm^{-1} bandwidth for the two vinyl bands at 1623 and 1631 cm^{-1}, respectively. The resulting depolarization ratios showed that the 1616 cm^{-1} band was depolarized, as expected for a mode of B_{1g} symmetry, but that the 1631 cm^{-1} band was polarized (A_{1g}) with both Soret and visible excitation. An ambiguous result was obtained for the other vinyl mode at 1624 cm^{-1}, owing to the overlap with the ν_{10} mode, and only an intermediate value for the polarization ratio could be obtained.

Proximal Histidine-Fe^{II} Linkage in Reduced HRP-C and the F41V and R38K Variants.* Figure 11 compares the low-frequency region of the RR spectra of the Fe^{II} forms of HRP-C*, F41V, and R38K obtained with Soret excitation. The data for the F41W variant are not shown since it was not possible to completely reduce this protein. Reduced HRP-C* gave a spectrum identical to that previously reported for the plant enzyme by Teraoka and Kitagawa (1981). It is characterized by a strong band at 243 cm^{-1}, which has been assigned to the bond stretch between Fe^{II} and the N_ϵ of the proximal imidazole (His170). Figure 11 also shows that replacement of Phe41 by Val does not significantly affect the frequency of the ν(Fe–Im) stretching mode. However, the R38K mutation causes a downshift of 3 cm^{-1}, indicating a weakening of the Fe–imidazole bond presumably due to the more neutral, less imidazolate character of the axial ligand.

The high-frequency region of the RR spectra of reduced HRP-C* was identical to those of previously reported Fe^{II} spectra of the plant enzyme (Kitagawa *et al.*, 1983). In common with the spectra of F41V and R38K (data not shown), strong bands were seen at 1469, 1563, and 1603 cm^{-1} corresponding to the ν_3, ν_2, and ν_{10} modes, respectively, of a normal 5-cHS heme (Choi *et al.*, 1982).

DISCUSSION

Ferric Hemes. In all of our measurements to date, the refolded, recombinant enzyme gave spectra that were identical to those reported previously with the plant enzyme. This confirms the conclusions from kinetic (Smith *et al.*, 1992) and NMR (Veitch *et al.*, 1992) measurements that the two enzymes, or more specifically their heme active sites, are indistinguishable. The folding and reconstitution procedure employed during the preparation of the recombinant enzyme from *E. coli* inclusion bodies (Smith *et al.*, 1990) therefore does not result in any detectable modification of the enzyme structure or its heme group.

The RR spectra of both the recombinant and the plant proteins show a splitting of the core size marker bands into two components, suggesting the existence of two forms that have been assigned to 5-c- and 6-cHS hemes. However, it should be noted that some bands appear at frequencies that differ considerably from those assigned to the corresponding model HS hemes. Therefore, prior to making assignments for any new bands observed in the RR spectra of HRP-C* variants, it is necessary to better understand the atypical frequencies of the core size marker bands, which are common features of the RR spectra of both plant and wild-type recombinant HRP-C. The anomalously high frequencies of the ν_3 modes have been observed previously in the spectra of HRP reported by other workers (Rakshit & Spiro, 1974; Teraoka & Kitagawa, 1981; Kitagawa *et al.*, 1983; Terner & Reed, 1984; Evangelista-Kirkup *et al.*, 1985; Palaniappan & Terner, 1989; Smulevich *et al.*, 1991b). However, Table 1 shows not only that the HS ν_3 modes are about 10 cm^{-1} higher for the 6-cHS and 5-cHS states of HRP compared to model compounds but also that ν_{19} and ν_{10} show the same behavior. Recently, Czernuszewicz *et al.* (1989) reported that flattening of the porphyrin ring in nickel octaethylporphyrin causes

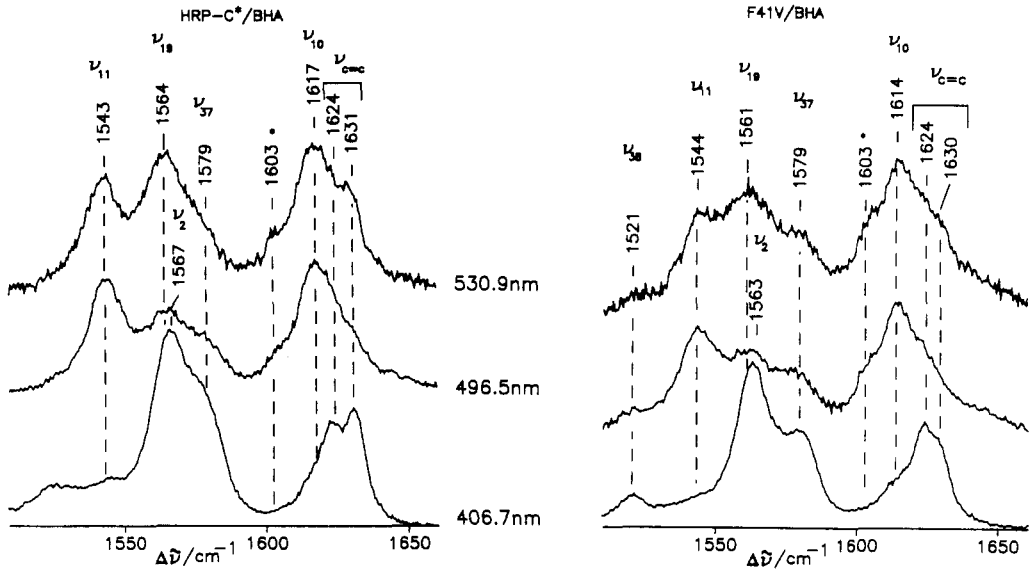

FIGURE 9: Resonance Raman spectra of the BHA-complexed forms of Fe^{III} HRP-C* (left) and the F41V variant (right) at pH 7.1 with various excitation wavelengths. Experimental conditions: 5-cm^{-1} resolution; 406.7-nm excitation, 3 s/0.5 cm^{-1} collection interval, and 30-mW laser power at the sample; 496.5-nm excitation, 25 s/0.5 cm^{-1} collection interval, and 70-mW laser power at the sample; 530.9-nm excitation, 32 s/0.5 cm^{-1} collection interval, and 70-mW laser power at the sample. The * indicates the band at 1605 cm^{-1} due to BHA.

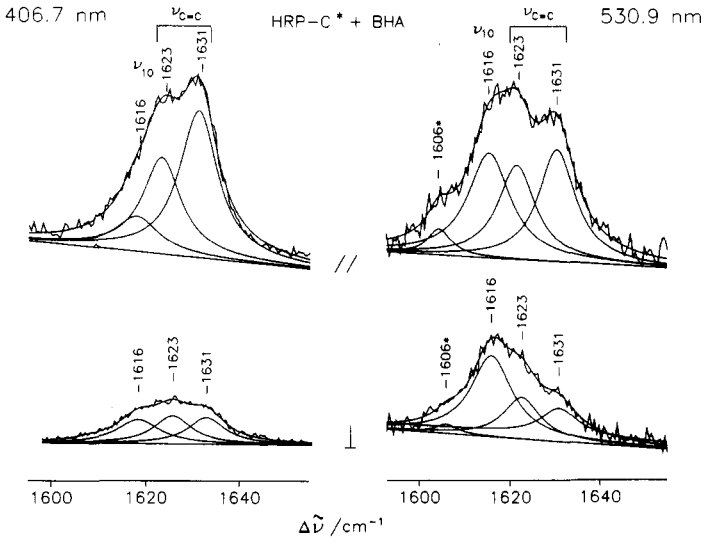

FIGURE 10: Resonance Raman and curve-fitted spectra of the ν_{10} and ν(C=C) stretching modes of the BHA complex of Fe^{III} recombinant HRP-C* in polarized light with 406.7- (left) and 530.9-nm (right) excitation. Experimental conditions are as given in the legend to Figure 8. The * indicates the band at 1605 cm^{-1} due to BHA.

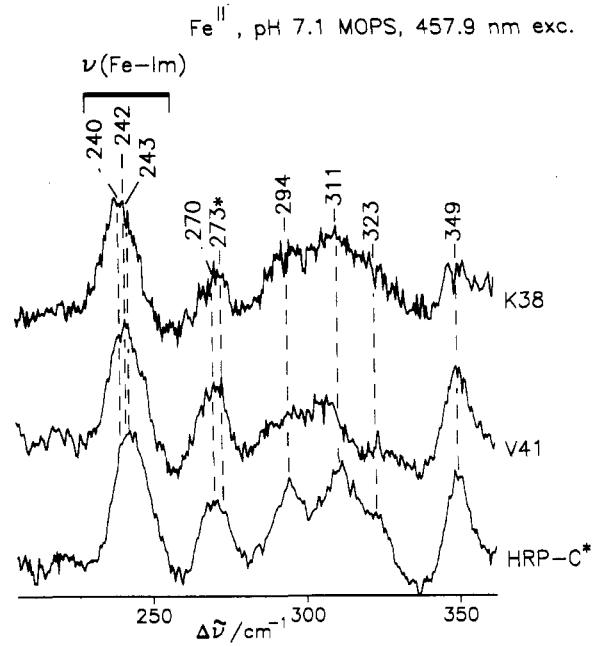

FIGURE 11: Resonance Raman spectra of Fe^{II} recombinant HRP-C* and the F41V and R38K variants at pH 7.1 recorded with 457.9-nm excitation, 5-cm^{-1} resolution, a 10 s/0.5 cm^{-1} collection interval, and 20-mW laser power at the sample. The * indicates a plasma line.

significant increases in some, but not all, of the core size marker bands. This is consistent with the proposal of Rakshit and Spiro (1974) that the HS heme in HRP may be more planar than in other heme proteins. This may account for the elevated frequencies of the asymmetric stretching of the C_a–C_m bridge bonds ν_3, ν_{10}, and ν_{19}, which are particularly sensitive to the out-of-plane displacement of the C_m atoms (Choi *et al.*, 1982).

Prendergast and Spiro (1992) investigated the responsiveness of metalloporphyrin skeletal mode vibrational frequencies to changes in both the core size and planarity of the macrocycle. They found that swiveling or tilting of the pyrrole rings, to produce ruffled or domed porphyrins, has nonnegligible kinematic consequences for the skeletal mode frequencies, especially for the ν_{10} and ν_{19} modes.

The magnetic moment of HRP-C (5.23 m_B) (Tamura, 1971; Schonbaum, 1973) also does not agree with that of a pure HS state (5.9 m_B; Maltempo *et al.*, 1979). This deviation has been interpreted in terms of a quantum mechanical admixture of Fe^{III} high- and intermediate-spin (IS) atoms. An analysis of the the RR spectra of IS model compounds has shown an increase in the frequencies of all of the core size marker bands in the 1450 and 1700 cm^{-1} regions (Teraoka & Kitagawa, 1980). In addition, HRP-C behaves differently from other heme proteins at low temperature. Whereas CCP gives rise to a mixture of HS and LS forms at 20 K (Smulevich *et al.*, 1989b; Yonetani & Anni, 1987), HRP-C gives rise to a mixture of LS and IS forms (Smulevich *et al.*, 1991; Tamura, 1971; Schonbaum, 1973).

It seems likely that the distortion of the porphyrin ring might result from external forces such as steric contacts with the protein. This effect is partially relieved upon complexation with BHA (see below) or mutation of the distal side chains at F41 or R38 sites. These changes cause the appearance of

Table 2: Coordination and Spin States of HRP, CCP, and Their Distal Side Variants[a]

HRP-C* (WT) (F41)	CCP(MI) (W51F)	HRP-C* (F41W)	CCP(MI)(WT) (W51)	HRP-C* (F41V)	HRP-C* (R38K)	CCP(MI) (R48K)
6-cHS#		6-cHS#		6-cHS#	6-cHS#	
	6-cHS	6-cHS		6-cHS	6-cHS	
5-cHS#		5-cHS#		5-cHS#	5-cHS#	
	5-cHS		5-cHS			
					6-cLS	6-cLS

[a] HS, high spin; LS, low-spin; 5-c, 5-coordinate; 6-c, 6-coordinate; # refers to a species showing core size marker bands with atypical frequencies with respect those observed for the corresponding heme model compounds. The underlined species indicates the prevalent species.

new species characterized by different core size marker band frequencies, which correspond to those of 6-cHS (V41 and W41) and 6-cLS (K38) model compounds. The X-ray structure of HRP-C is not yet available, but on the basis of the high-resolution structure of CCP, which contains a distal water molecule above the Fe atom (H_2O 595, not coordinated to the iron in the resting enzyme), a plausible candidate for the sixth ligand would be a corresponding water molecule molecule in HRP-C. One of the recently solved low-pH structures of lignin peroxidase (Piontek *et al.*, 1993) reveals the presence of a distal water molecule coordinated at the sixth position.

The heme pocket architectures of HRP-C and CCP appear significantly different on the distal side. At neutral pH, baker's yeast CCP, which contains a Trp in position 51, is mainly 5-cHS (Dasgupta *et al.*, 1989; Hashimoto *et al.*, 1986), whereas the W51F mutant is predominantly 6-cHS. Smulevich *et al.* (1988a) concluded that in CCP the loss of the H-bond between the Trp51 and H_2O 595 allows the distal water molecule to coordinate to the heme Fe. HRP-C has a Phe residue at position 41, but still contains a mixture of predominantly 5- and some 6-cHS hemes. However, the relative abundance of the two heme forms is reversed with respect to that of the CCP(MI) W51F mutant. The HRP-C F41W variant is characterized by an increase in the amount of 6-cHS heme at the expense of the 5-cHS# species. This effect is even more pronounced in the F41V mutant. Therefore, replacement of Phe41 with Trp in HRP gives rise to the opposite effect compared to wild-type CCP (Table 2).

Goodin *et al.* (1991) showed that CCP variants at the corresponding position, Trp51, result in a number of significant effects on the kinetics and coordination state of the enzyme, presumably caused by significant conformational perturbation of the distal side of the heme pocket and the water structure within it. The absorption spectra of the variants were characteristic of predominantly 6-cHS (W51M, W51T, and W51A) or -LS (W51C and W51G) hemes. None of the variants showed any signs of a 5-cHS form. Therefore, in the case of CCP, the presence of the H-bond between the indole side chain of Trp51 and the distal water molecule (595) appears to be important for restraining the distal water molecule and preventing it from binding to the sixth coordination position of the Fe atom. The present results with HRP-C variants suggest that, within the spatial constraints of the HRP-C heme pocket, a Trp side chain at position 41 cannot restrain a distal water molecule as it does in wild-type CCP. This must be due in part either to a different disposition of the distal residues and/or to a different distance or arrangement of distal water molecules in the heme cavity (possibly less space and, therefore, less water molecules in the distal cavity).

Replacement of Arg38 in HRP-C gives rise to the appearance of some 6-cLS heme, a result similar to that obtained previously for the corresponding mutant of CCP, R48K. The crystallographic structure of CCP(R48K) (Vitello *et al.*, 1993) shows that Lys48 moves toward the heme iron, displacing the distal water molecule (595), and occupies the peroxide binding site. It appears that the ϵ-amino group of Lys48 does not bind the heme iron, but the electronic absorption (Vitello *et al.*, 1993) as well as the RR spectra at pH 6 (Smulevich *et al.*, 1988a) suggest that the protein contains a small proportion of a hexacoordinate low-spin component, which was attributed to distal ligation by the Lys amine side chain (Smulevich *et al.*, 1988a). The electronic absorption spectrum is dependent upon pH, and the protein shows the typical alkaline form of CCP with an apparent pK_a of 6.9. In this latter case, the low-spin species was attributed to distal ligation by the Lys amine side chain. The HRP-C variant R38K can exist in a number of pH-dependent interconvertible forms (Sanders *et al.*, 1993), and at pH 7.0 it exists as mixture of three forms. Further work will be required to determine which of these forms contributes to the LS signals observed in this work.

Effect of BHA. By comparing the spectra obtained in the presence and absence of BHA (Figure 2), pronounced effects can be detected for HRP-C and the F41V variant, but not for the R38K and F41W variants. These results were mirrored in the absorption spectra of the BHA:HRP variant complexes (data not shown). Binding of BHA causes a dramatic change in the absorption spectra of HRP (Schonbaum, 1973) and F41V (Smith *et al.*, 1992). The Soret band narrows and the maximum shifts from 403 to 408–407 nm in the BHA complex, giving rise to a spectrum characteristic of a 6-cHS heme. However, there were no detectable changes in the spectra of either R38K or F41W upon addition of the donor (data not shown). Smith *et al.* (1993) showed that neither R38K nor F41W was retained during chromatography on a BHA–Sepharose affinity column unlike the wild type, suggesting that the binding site for this donor had been destroyed in these two variants.

The RR spectra of the wild-type and recombinant HRP-C:BHA complexes are characterized by the appearance of new bands due to a 6-cHS species. The bands due to the 6-cHS# form remained after BHA binding, while the 5-cHS# species completely disappeared. Therefore, the proportion of 6-cHS heme grows at the expense of the 5-c form. The magnetic moment of the wild-type HRP-C shifts from 5.23 to 5.97 m_B on binding BHA at room temperature, and the EPR spectrum shows only HS signals (Schonbaum, 1973). In agreement, the low-temperature RR spectra (Smulevich *et al.*, 1991b) are characterized by core size marker bands corresponding to 6-cHS# (ν_3 at 1491 cm^{-1}, ν_{11} at 1547 cm^{-1}, ν_2 at 1569 cm^{-1}, ν_{19} at 1567 cm^{-1}, and ν_{10} at 1616 cm^{-1}).

The binding of BHA to the F41V variant gives rise to a higher population of the 6-cHS heme. This is probably simply due to the fact that the proportion of 6-cHS# heme of the resting mutant protein is already substantially less than that of wild-type HRP-C. The spectra of HRP-C* and F41V also differ in the relative intensity of the bands due to the ν(C=C) at 1630 and 1624 cm^{-1}, the latter being much more intense for the F41V variant. The increase in intensity of this band has been observed previously for HRP-C, together with a strong enhancement of the E_u mode at 1579 cm^{-1} (Smulevich *et al.*, 1991b). On the basis of the present results, it seems

that the intensity of the vinyl band at 1624 cm^{-1} can be correlated with the amount of 6-cHS form.

On the basis of NMR studies on HRP-C (Sakurada *et al.*, 1986; Thanabal *et al.*, 1987a,b), the substrate binding site has been proposed to be close to the C18 methyl group of the heme. A recent NMR study on the interaction between cyanide-ligated HRP-C and BHA detected chemical shift perturbations to protons of the distal His42 and Arg38, with NOE connectivities established between His42 C_ϵ^1H and protons of the BHA aromatic nucleus (Veitch *et al.*, 1992, 1993). This information confirms that the binding site lies toward the distal rather than the proximal side of the heme. The RR data indicate that the occupation of this site by BHA gives rise to a mixture of two 6-cHS forms, which differ in the degree to which their hemes are distorted. This result seems to be consistent with the findings of La Mar *et al.* (1993) based on NMR of HRP-CN, who detected two components in the heme methyl C18 resonance during titration with BHA. These results were interpreted in terms of a major and a minor mode of binding. The RR spectra of the V41:BHA complex show only a very small contribution from a 6-cHS# heme. This variant has a 2-fold higher affinity for BHA relative to the wild type and a modified reactivity toward H_2O_2 and reducing substrates such as *p*-aminobenzoic acid (Smith *et al.*, 1992).

Interestingly, the F41W variant does not appear to bind BHA (Smith *et al.*, 1993; this work), whereas F41V does (Smith *et al.*, 1992). It is not easy at this stage to give a precise explanation for this difference in behavior. Clearly, distal site mutations (including R38K; Smith *et al.*, 1993), which have the potential to disrupt the heme-linked hydrogen-bonding network, can abolish the binding of BHA. This is in line with the suggestion based on NMR data (Veitch *et al.*, 1993) that hydrogen-bonding interactions are important for the binding of this ligand. The NMR data of La Mar *et al.* (1993) favor a direct hydrogen-bonding interaction with the distal histidine, while modeling studies (Smith *et al.*, 1993) were interpreted as suggesting that hydrogen-bonding interactions to the the distal Arg were more likely.

Ferrous Hemes. At neutral pH, the reduced forms of all of the recombinant HRP-Cs discussed above contain a 5-coordinate high-spin heme (5-cHS), as does the wild-type plant HRP-C (Kitagawa *et al.*, 1983). The low-frequency regions of RR spectra of the Fe^{II} forms of HRP-C are characterized by a strong band at 243 cm^{-1}, which has been assigned to the stretching of the bond between the Fe^{II} and the proximal imidazole side chain of His170 (Teraoka & Kitagawa, 1981). The high frequency of this mode has been interpreted as reflecting the imidazolate character of the axial ligand, induced by a polar $N^-\cdots HO$ hydrogen bond between the axial ligand (His170) and a buried Asp side chain (probably Asp247). The presence of this hydrogen bond is a characteristic of all plant and animal peroxidases studied so far (Kimura *et al.*, 1981; Teraoka & Kitagawa 1981; Kitagawa *et al.*, 1983; Desbois *et al.*, 1984; Kuila *et al.*, 1985; Hashimoto *et al.*, 1986; Manthey *et al.*, 1986; Smulevich *et al.*, 1988a, 1991a; Dasgupta *et al.*, 1989; Spiro *et al.*, 1990). It has been suggested to have a general role in maintaining the imidazolate nature of the axial ligands, allowing it to stabilize the high oxidation state intermediates of the heme iron.

The replacement of Phe41 with Val does not affect the frequency of the ν(Fe–Im) stretching mode, but the mutation in position 38 causes a 3 cm^{-1} downshift of this band, suggesting a weakening in the Fe–Im bond strength. A similar perturbation has been observed for the Leu48 mutant of CCP, whereas Lys48 and Phe51 variants (analogous to residues in positions 38 and 41 in the sequence of HRP-C) show essentially the same spectra as CCP (Smulevich *et al.*, 1988a). Detailed resonance Raman studies of different distal and proximal mutants of CCP at different pH's have shown that the His175–Asp235 interaction is sensitive to long-range effects due to the presence of a hydrogen-bond network connecting the proximal and distal sides of the heme through Trp51–Arg48–heme propionate–His181 residues. In HRP, some of the key elements of this network, namely, Arg38, His170, and Asp247, are conserved. Therefore, the downshift of the ν(Fe–Im) stretching mode observed for the R38K mutant suggests the presence of such a hydrogen-bond connection in HRP-C too, in line with the suggestion of Veitch *et al.* 1992). These RR studies are therefore in agreement with earlier NMR studies of HRP-C*R38K (Veitch *et al.*, 1992) which suggested a more neutral heme-coordinated histidine imidazole ring in this variant.

CONCLUSIONS

The folding and reconstitution procedure employed during the preparation of the recombinant HRP-C from *E. coli* inclusion bodies does not result in any detectable modification to the enzyme structure or its heme group.

The RR spectra of both the recombinant and the plant proteins show a splitting of the core size marker bands into two components, suggesting the existence of two forms assigned to a 5 and 6-c HS. Some bands, namely the ν_3 and ν_{10} appear at considerable higher frequencies, than those assigned for the corresponding model HS hemes. This discrepancy is attributed to a different degree of distortion of the heme from planarity in HRP-C, resulting from external forces such as steric contacts with the protein.This effect is partially relieved upon complexation with BHA or by mutation of the distal side chains of F41 or R38, both complexation and mutation presumably perturb the heme-linked H-bonding network.

The HRP-C F41W and F41V variants are characterized by an increase in the amount of 6-c HS heme at the expense of the 5-c HS species; the R38K by an increase in both 6-c HS and LS hemes. By comparing these results with those reported previously for the corresponding CCP mutants, it appears that HRP-C differs from CCP in having an altered structure of the distal water molecules in the heme cavity. The H-bonding network coupling the distal and the proximal sides of the heme appears to be conserved between HRP-C and CCP.

Mutations in the distal side of the pocket also affect the ability of the protein to bind BHA. The RR spectra of HRP-C:BHA complex indicate that a mixture of two 6-c HS hemes are present when this donor is bound to the enzyme. F41W and R38K mutants loose their capability to bind the substrate, whereas the F41V variant has a two-fold higher affinity. These data are consistent with the aromatic donor binding site lying toward the distal rather than the proximal side of the heme.

REFERENCES

Bosshard, H. R., Anni, H., & Yonetani, T. (1991) in *Peroxidases in Chemistry and Biology* (Everse, J., Everse, K. E., & Grisham, M. B., Eds.) Vol. II, pp 51–84, CRC Press, Boca Raton, FL.

Choi, S., Spiro, T. G., Langry, K. C., Smith, K. M., Budd, D. L., & La Mar, G. N. (1982) *J. Am. Chem. Soc. 104*, 4345.

Czernuszewicz, R. S., Li, X. Y., & Spiro, T. G. (1989) *J. Am. Chem. Soc. 111*, 7024.

Dasgupta, S., Rousseau, D. L., Anni, H., & Yonetani, T. (1989) *J. Biol. Chem. 264*, 654.

Desbois, A., Mazza, G., Stetzkowski, F., & Lutz, M. (1984) *Biochim. Biophys. Acta 785*, 161.

de Ropp, J. S., & La Mar, G. N. (1991) *J. Am. Chem. Soc. 113*, 4348.
de Ropp, J. S., La Mar, G. N., Smith, K. M., & Langry, K. C. (1984) *J. Am. Chem. Soc. 106*, 4438.
de Ropp, J. S., Yu, L. P., & La Mar, G. N. (1991) *J. Biomol. Nucl. Magn. Reson. 1*, 175.
Dunford, H. B. (1991) in *Peroxidases in chemistry and biology* (Everse, J., Everse, K. E., & Grisham, M. B., Eds.) Vol. II, pp 1–24, CRC Press, Boca Raton, FL.
Dunford, H. B., & Stillman, J. S. (1976) *Coord. Chem. 19*, 187.
Edwards, S. L., Xuong, N., Hamlin, R. C., & Kraut, J. (1987) *Biochemistry 26*, 1503.
Edwards, S. L., Raag, R., Wariishi, H., Gold, M., & Poulos, T. L. (1993) *Proc. Natl. Acad. Sci. U.S.A. 90*, 750.
Erman, J. E., Vitello, L. B., Miller, M. A., & Kraut, J. (1992) *J. Am. Chem. Soc. 114*, 6592.
Evangelista-Kirkup, R., Grisanti, M., Poulos, T. L., & Spiro T. G. (1985) *FEBS Lett. 190*, 221.
Finzel, B. C., Poulos, T. L., & Kraut, J. (1984) *J. Biol. Chem. 259*, 13027.
Goodin, D. B., Davidson, M. G., Roe, J. A., Mauk, G., & Smith, M. (1991) *Biochemistry 30*, 4953.
Hashimoto, S., Teraoka, S., Inubushi, T., Yonetani, T., & Kitagawa, T. (1986) *J. Biol. Chem. 261*, 11110.
Hendra, P. J., & Loader, E. J. (1968) *Chem. Ind. (London)*, 718.
Henriksen, A., Svensson, L. A., Smith, A. T., Burke, J. F., Thorneley, R. N. F., Welinder, K. G., & Gajhede, M. (1993) in *Plant Peroxidases Biochemistry and Physiology, III International symposium proceedings* (Welinder, K. G., Rasmussen, S. K., Penel, C., & Greppin, H., Eds.) pp 5–8, University of Geneva, Geneva, Switzerland.
Kersten, P. J., Kalyanaraman, B., Hammel, K. E., Reinhammar, B., & Kirk, T. K. (1990) *Biochem. J. 268*, 475.
Kimura, S., Yamazaki, I., & Kitagawa, T. (1981) *Biochemistry 20*, 4632.
Kitagawa, T., Hashimoto, S., Teraoka, J., Nakamura, S., Yajima, H., & Toichiro, H. (1983) *Biochemistry 22*, 2788.
Kuila, D., Tien, M., Fee, J. A., & Ondrias, M. R. (1985) *Biochemistry 24*, 3394.
Kunishima, N., Fukujama, K., Matsubara, H., Hatanaka, H., Shibano, Y., & Amachi, T. (1994) *J. Mol. Biol. 235*, 331.
La Mar, G. N., Hermandez, G., & de Ropp, J. S. (1993) *Biochemistry 31*, 9158.
Maltempo, M. M., Ohlsson, P.-I., Paul, K.-G., Petersson, L., & Ehrenberg, A. (1979) *Biochemistry 18*, 2935.
Manthey, J. A., Boldt, N. J., Bocian, D. F., & Chan, S. I. (1986) *J. Biol. Chem. 261*, 6734.
Morita, Y., Mikami, B., Yamashita, H., Lee, J. Y., Aibara, S., Sato, M., Katsube, Y., & Tanaka, N. (1991) in *Biochemical, Molecular and Physiological Aspects of Plant Peroxidases* (Lobarzewski, J., Greppin, H., Penel, C., & Gaspar, T., Eds.) pp 81–88, University of Geneva, Geneva, Switzerland.
Morita, Y., Funatsu, J., & Mikami, B. (1993) in *Plant Peroxidases Biochemistry and Physiology, III International Symposium Proceedings* (Welinder, K. G., Rasmussen, S. K., Penel, C., & Greppin, H., Eds.) pp 1–4, University of Geneva, Geneva, Switzerland.
Palaniappan, V., & Terner, J. (1989) *J. Biol. Chem. 264*, 16046.
Piontek, K., Glumoff, T., & Winterhalter, K. H. (1993) *FEBS Lett. 315*, 119 .
Poulos, T. L., & Kraut, J. (1980) *J. Biol. Chem. 255*, 8199.
Poulos, T. L., Edwards, S., Wariishi, H., & Gold H. M. (1993) *J. Biol. Chem. 268*, 4429.
Prendergast, K., & Spiro T. G. (1992) *J. Am. Chem. Soc. 114*, 3793.
Rakshit, G., & Spiro, T. G. (1974) *Biochemistry 13*, 5317.
Sakurada, J., Takahashi, S., & Hosoya, T. (1986) *J. Biol. Chem. 261*, 9657.
Sanders, S. A., Bray, R. C., & Smith, A. T. (1994) *Eur. J. Biochem.* (submitted for publication).
Saunders, S., & Burke, J. F. (1990) *Nucleic Acids Res. 18*, 4948.
Schombaum, G. R. (1973) *J. Biol. Chem. 248*, 502.
Smith, A. T., Santama, N., Dacey, S., Edwards, M., Bray, R. C., Thorneley, R. N. F., & Burke, J. F. (1990) *J. Biol. Chem. 265*, 1335.
Smith, A. T., Sanders, S. A., Thorneley, R. N. F., Burke, J. F., & Bray, R. C. (1992) *Eur. J. Biochem. 207*, 507.
Smith, A. T., Sanders, S. A., Sampson, C., Bray, R. C., Burke, J. F., & Thorneley, R. N. F. (1993) in *Plant Peroxidases Biochemistry and Physiology, III International symposium proceedings* (Welinder, K. G., Rasmussen, S. K., Penel, C., & Greppin, H., Eds.) pp 159–168, University of Geneva, Geneva, Switzerland.
Smulevich, G. (1993) in *Advances in Spectroscopy, Vol. 20: Biomolecular Spectroscopy* (Clark, R. J. H., & Hester, R. E., Eds.) pp 163–193, John Wiley, London.
Smulevich, G., Mauro, J. M., Fishel, L. F., English, A. M., Kraut, J., & Spiro, T. G. (1988a) *Biochemistry 27*, 5477.
Smulevich, G., Mauro, J. M., Fishel, L. F., English, A. M., Kraut, J., & Spiro, T. G. (1988b) *Biochemistry 27*, 5486.
Smulevich, G., Miller, M. A., Gosztola, D., & Spiro, T. G. (1989a) *Biochemistry 28*, 3960.
Smulevich, G., Mantini, A. R., English, A. M., & Mauro, J. M. (1989b) *Biochemistry 28*, 5058.
Smulevich, G., Wang, Y., Edwards, S. L., Poulos, T. L., English, A. M., & Spiro, T. G. (1990a) *Biochemistry 29*, 2586.
Smulevich, G., Wang, Y., Mauro, J. M., Wang, J., Fishel, L. A., Kraut, J., & Spiro, T. G. (1990b) *Biochemistry 29*, 7174.
Smulevich, G., Miller, M. A., Kraut J., & Spiro, T. G. (1991a) *Biochemistry 30*, 9546.
Smulevich, G., English, A. M., Mantini, A. R., & Marzocchi, M. P. (1991b) *Biochemistry 30*, 772.
Spiro, T. G., & Li, X. Y. (1988) in *Biological Applications of Raman Spectroscopy, Volume 3: Resonance Raman Spectra of Heme and Metalloproteins* (Spiro, T. G., Ed.) pp 1–37, John Wiley, New York.
Spiro, T. G., Smulevich, G., & Su, C. (1990) *Biochemistry 29*, 7174.
Tamura, M. (1971) *Biochim. Biophys. Acta 243*, 249.
Teraoka, J., & Kitagawa, T. (1980) *J. Phys. Chem. 84*, 1928.
Teraoka, J., & Kitagawa, T. (1981) *J. Biol. Chem. 256*, 3969.
Terner, J., & Reed, D. E. (1984) *Biochim. Biophys. Acta 789*, 80.
Thanabal, V., de Ropp, J. S., & La Mar, G. N. (1987a) *J. Am. Chem. Soc. 109*, 265.
Thanabal, V., de Ropp, J. S., & La Mar, G. N. (1987b) *J. Am. Chem. Soc. 109*, 7516.
Thanabal, V., de Ropp, J. S., & La Mar, G. N. (1988) *J. Am. Chem. Soc. 110*, 3027.
Veitch, N. C., Williams, R. J. P., Bray, R. C., Burke, J. F., Sanders, S. A., Thorneley, R. N. F., & Smith, A. T. (1992) *Eur. J. Biochem. 207*, 521.
Veitch, N. C. (1993) in *Plant Peroxidases Biochemistry and Physiology, III International Symposium Proceedings* (Welinder, K. G., Rasmussen, S. K., Penel, C., & Greppin, H., Eds.) pp 57–64, University of Geneva, Geneva, Switzerland.
Vitello, L. B., Erman, J. E., Miller, M. A., Wang, J., & Kraut, J. (1993) *Biochemistry 32*, 9807.
Welinder, K. G. (1985) *Eur. J. Biochem. 151*, 497.
Welinder, K. G. (1992) *Curr. Opin. Struct. Biol. 2*, 388.
Yonetani, T., & Anni, H. (1987) *J. Biol. Chem. 262*, 9547.